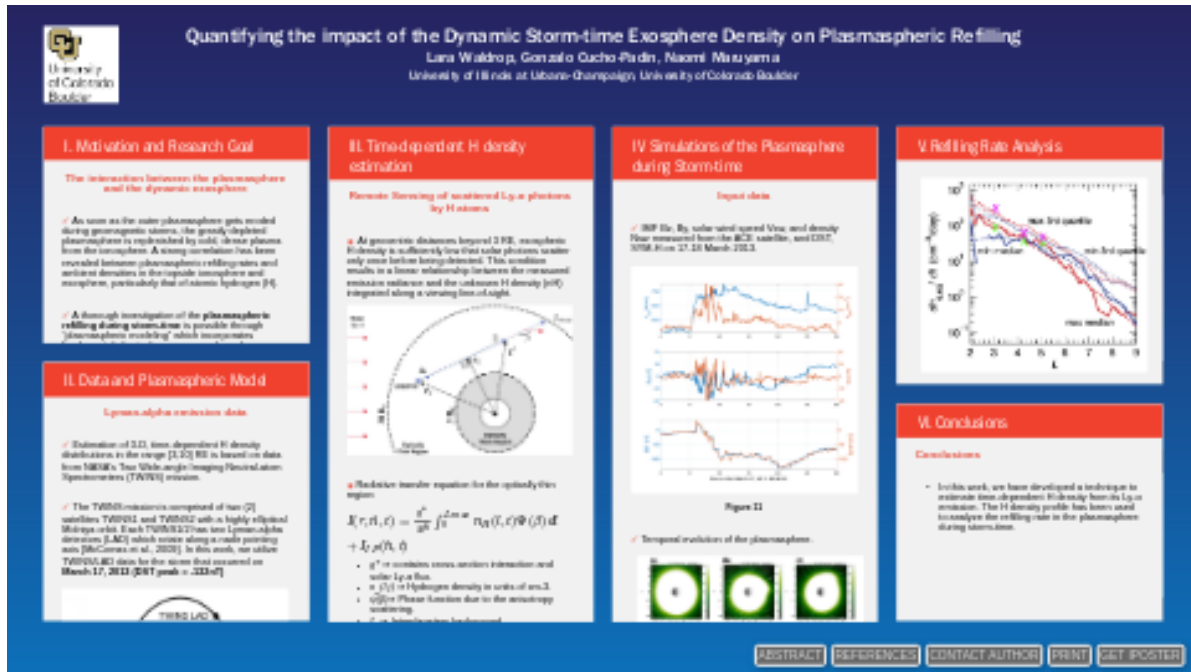


Quantifying the impact of the Dynamic Storm-time Exosphere Density on Plasmaspheric Refilling



Lara Waldrop [1], Gonzalo Cucho-Padin [1], Naomi Maruyama [2]

[1] University of Illinois at Urbana-Champaign, [2] University of Colorado Boulder

Contact: gac3@illinois.edu

PRESENTED AT:



I. MOTIVATION AND RESEARCH GOAL

The interaction between the plasmasphere and the dynamic exosphere

● As soon as the outer plasmasphere gets eroded during geomagnetic storms, the greatly depleted plasmasphere is replenished by cold, dense plasma from the ionosphere. A strong correlation has been revealed between plasmaspheric refilling rates and ambient densities in the topside ionosphere and exosphere, particularly that of atomic hydrogen (H) [Kral et al., 2018 (<http://agupubs.onlinelibrary.wiley.com/doi/full/10.1002/2017SW001780>)].

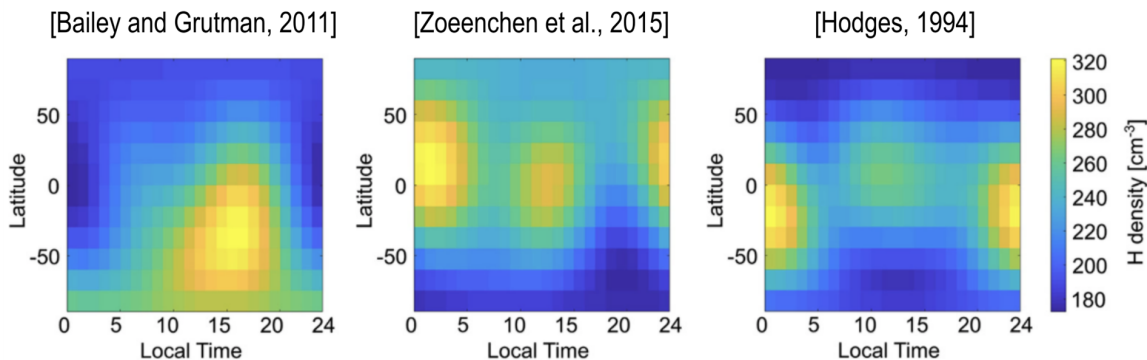
● A thorough investigation of the **plasmaspheric refilling during storm-time** is possible through “plasmaspheric modeling” which incorporates fundamental physical processes such as charge-exchange, ion-ion collisions, and wave-particle interactions. However, its accuracy **depends critically on the specification of the exospheric H density distributions**.

● The terrestrial exosphere is the uppermost layer of the atmosphere which extends from 500 km (exobase) up to $\sim 30 R_E$ (Earth radii). The atomic hydrogen (H) is the main constituent.

● **Remote sensing of solar Lyman-alpha photon scattered by exospheric H atoms (“Ly- α ” @ 121.6nm)** is the only means available to estimate exospheric density distributions over such a vast region.

● Existing theoretical and data-based H density models have been generated **specifically for quiet-time conditions** whereby the assumption of a static exosphere is likely valid.

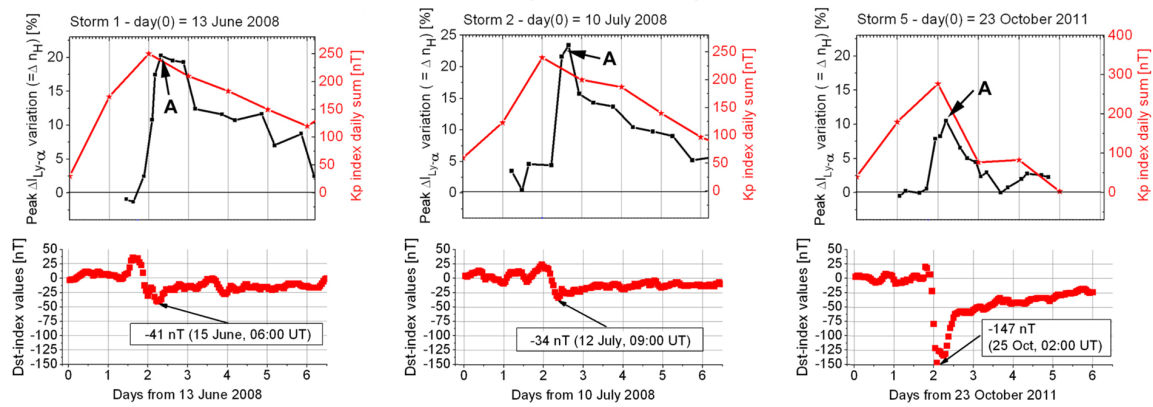
Hydrogen density distribution for a given radial shell $R = 3.2 R_E$



● Recent observations of Ly- α emission scattered by exospheric H atoms unveiled the **rapid fluctuations in their density distributions during geomagnetic storms** [Zoeenchen et al., 2017 (<https://doi.org/10.5194/angeo-35-171-2017>), Kuwabara et al., 2017 (<https://agupubs.onlinelibrary.wiley.com/doi/full/10.1002/2016JA023247>)]. Such a dynamic behavior is yet to be included in those H density models.

Scattered Lyman-alpha (@121.6nm) variation during storm time

Source: [Zoenenchen et al., 2017]



Overarching question

What is the role of the storm-time terrestrial exosphere on the plasmaspheric refilling rate?

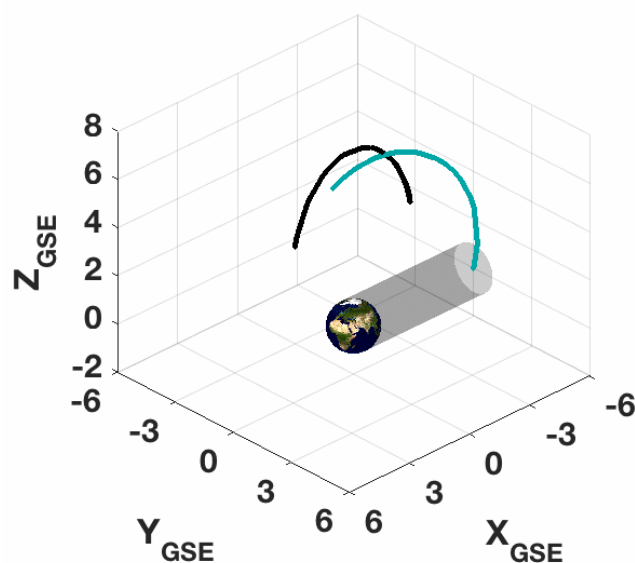
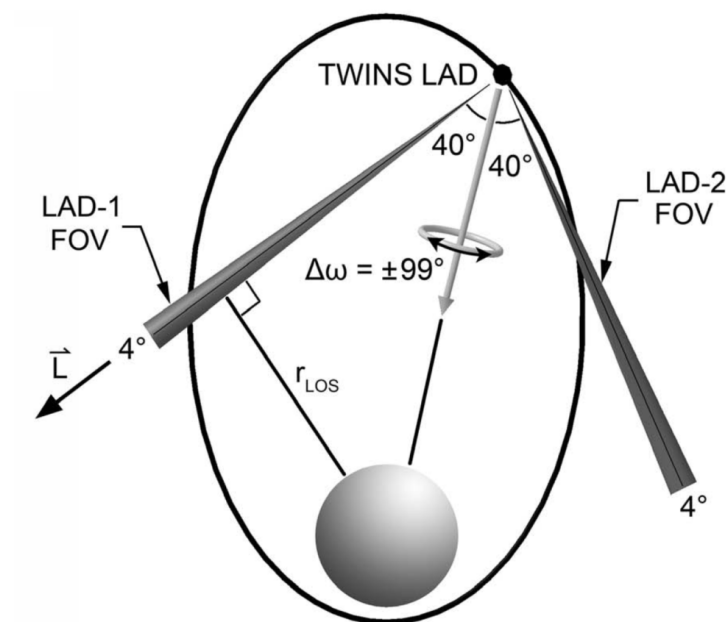
- To address this question, we estimate the 3-D, time-dependent hydrogen density distributions based on its Ly- α emission and a tomographic approach during storm-time. We then include the retrieved H density profile into a plasmasphere model and assess the refilling rate.

II. DATA AND PLASMASPHERIC MODEL

Lyman-alpha emission data

● Estimation of 3-D, time-dependent H density distributions is based on data from NASA's Two Wide-angle Imaging Neutral-atom Spectrometers (TWINS) mission [McComas et al., 2009 (<http://doi.org/10.1007/s11214-008-9467-4>)]:

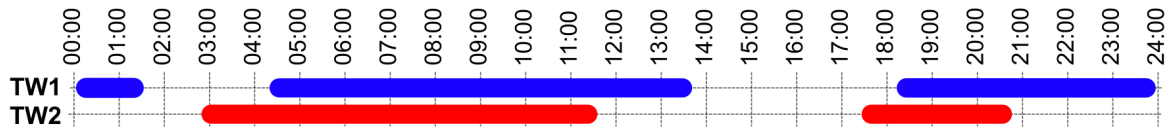
- TWINS mission is comprised of two satellites TWINS1/2.
- Each satellite has two Lyman-alpha detectors (LAD1/2)
- We utilize data for the storm that occurred on **March 17, 2013 (DST peak = -132nT)**
- Estimation range: [3,12] R_E geocentric distance.



Left panel from [Bailey and Grutman, 2011 (<https://doi.org/10.1029/2011JA016531>)]

- TWINS data availability is not continuous during the day.

TWINS data availability during March 17, 2013

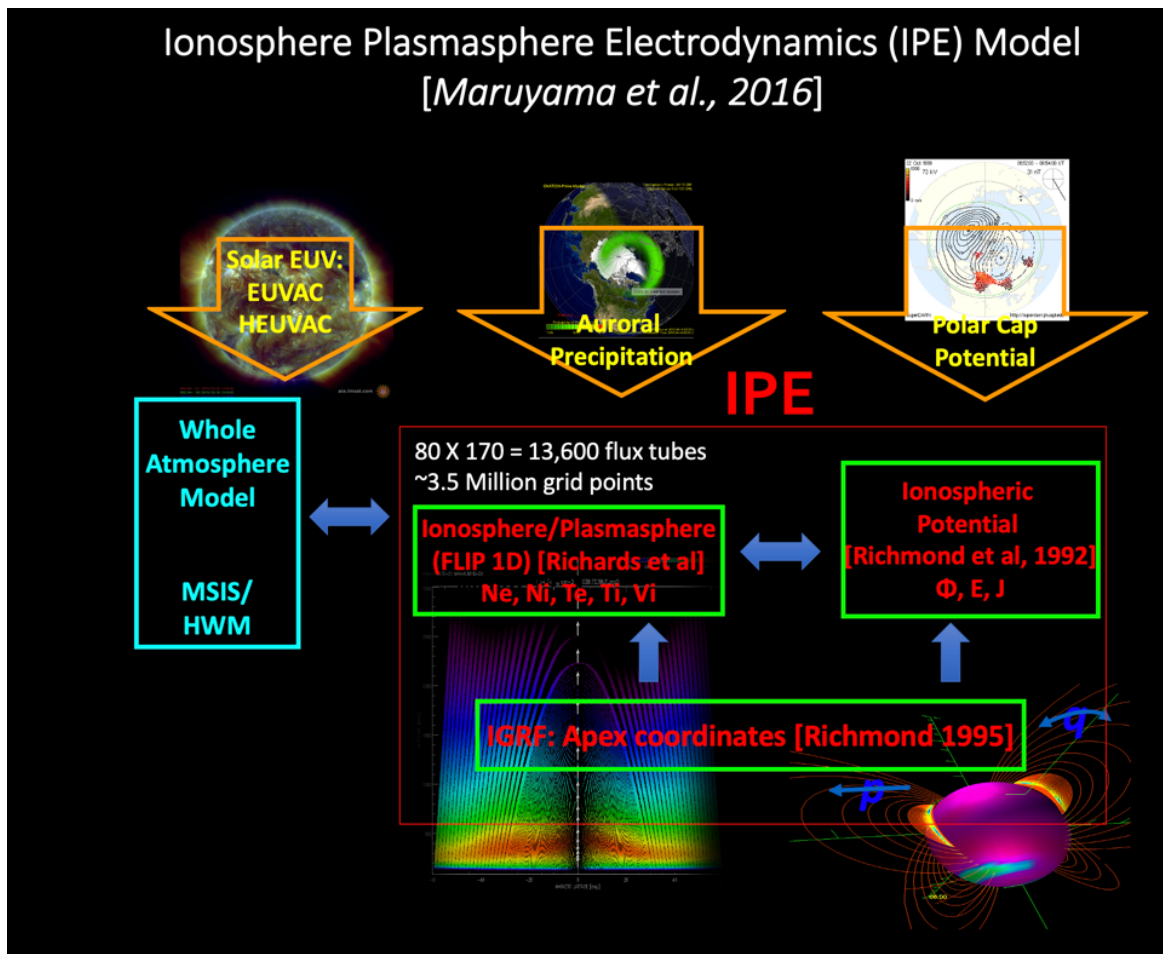


- Additionally, we use data from the Global UltraViolet Imager (GUVI) on-board the Thermosphere Ionosphere Mesosphere Energetics and Dynamics (TIMED) mission to estimate an averaged and spherically symmetric H density distribution during solar-maximum conditions in the region [92, 500] km [Qin et al, 2017 (<https://doi.org/10.1002/2017JA024489>)]

- We connect both datasets (GUVI and TWINS) using a two-exponential function based on a similar procedure demonstrated by [Østgaard et al., 2003 (<https://doi.org/10.1029/2002JA009749>)] using GEO/IMAGE data.

Plasmaspheric Model

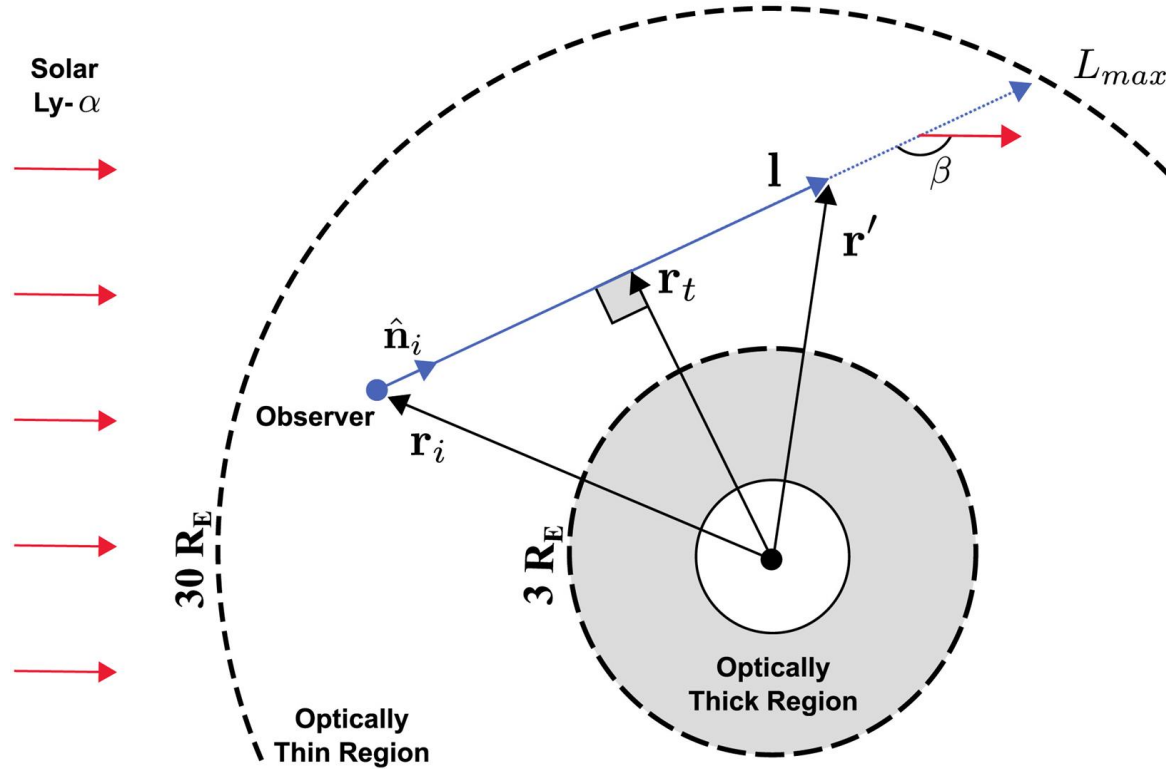
- We use the Ionosphere-Plasmasphere Electrodynamics (IPE) model to simulate the plasmaspheric dynamics.



III. TIME-DEPENDENT H DENSITY ESTIMATION

Remote sensing of scattered Ly- α photons by H atoms

● At geocentric distances beyond $3 R_E$, exospheric H density is sufficiently low that solar photons scatter only once before being detected. This condition results in a **linear relationship** between the measured emission radiance and the unknown H density (n_H) integrated along a viewing line-of-sight.

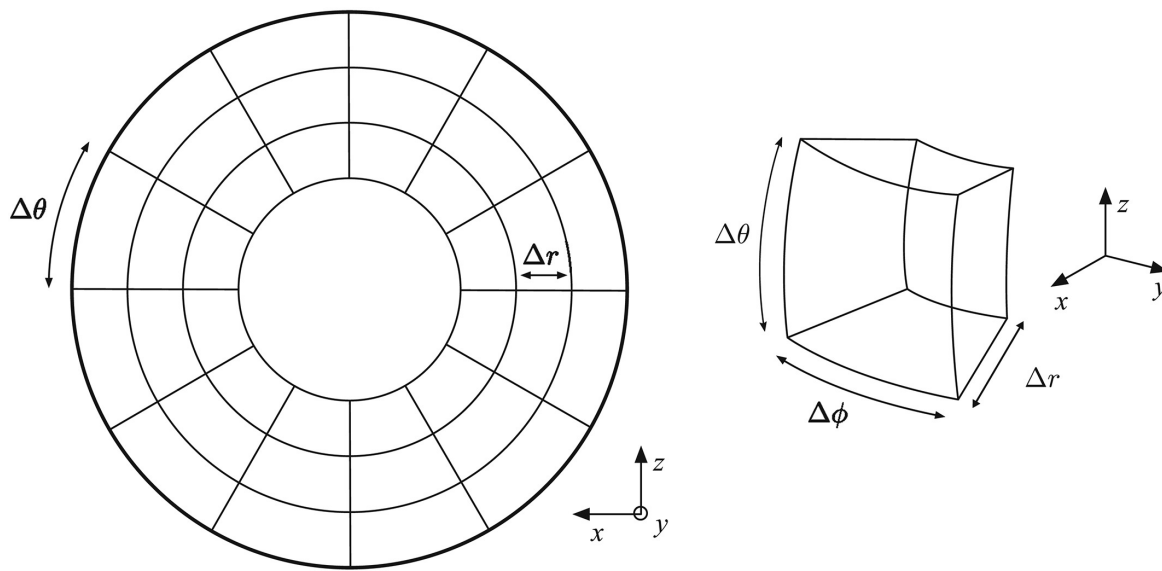


● Radiative transfer equation for the optically thin region:

$$I(r, \hat{n}, t) = \frac{g^*}{10^6} \int_0^{L_{max}} n_H(l, t) \Psi(\beta) dl + I_{IP}(\hat{n}, t)$$

- $g^* \Rightarrow$ contains cross-section interaction and solar Ly- α flux.
- $n_H(l, t) \Rightarrow$ Hydrogen density in units of cm^{-3} .
- $\psi(\beta) \Rightarrow$ Phase function due to the anisotropy scattering.
- $I_{IP} \Rightarrow$ Interplanetary background.
- $n_i \Rightarrow$ LOS direction.
- $r \Rightarrow$ Tangential distance of a LOS.

● The tomographic approach states that the volume of interest should be divided into voxels with a constant H density number. In this work, we adopt $\Delta r = 0.3125 R_E$, $\Delta \theta = 15 \text{ deg}$ and $\Delta \phi = 15 \text{ deg}$ yielding 6912 spherical voxels.



● After the spatial discretization into spherical voxels is performed, the radiative transfer equation adopts the form:

$$\mathbf{y} = \mathbf{L}\mathbf{x}$$

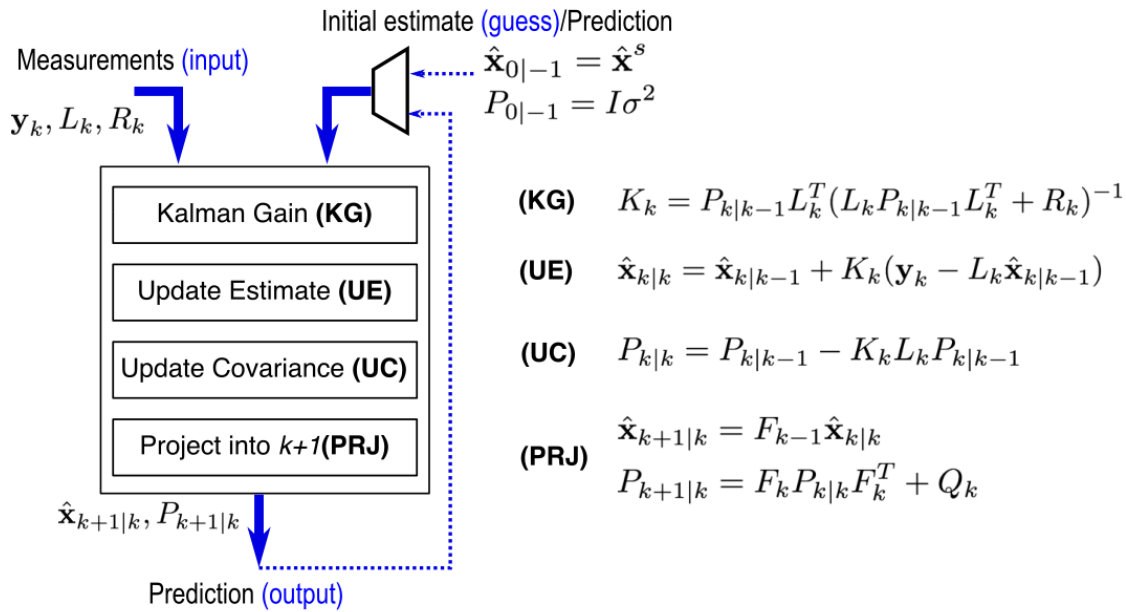
where:

- $\mathbf{y} \Rightarrow$ (known) the measurement vector generated by $I-I_P$
- $\mathbf{L} \Rightarrow$ (known) the observation matrix generated with LOS direction, satellite position, voxel dimension and solar Ly- α flux data.
- $\mathbf{x} \Rightarrow$ (unknown) the vector that contains the H density number per voxel.

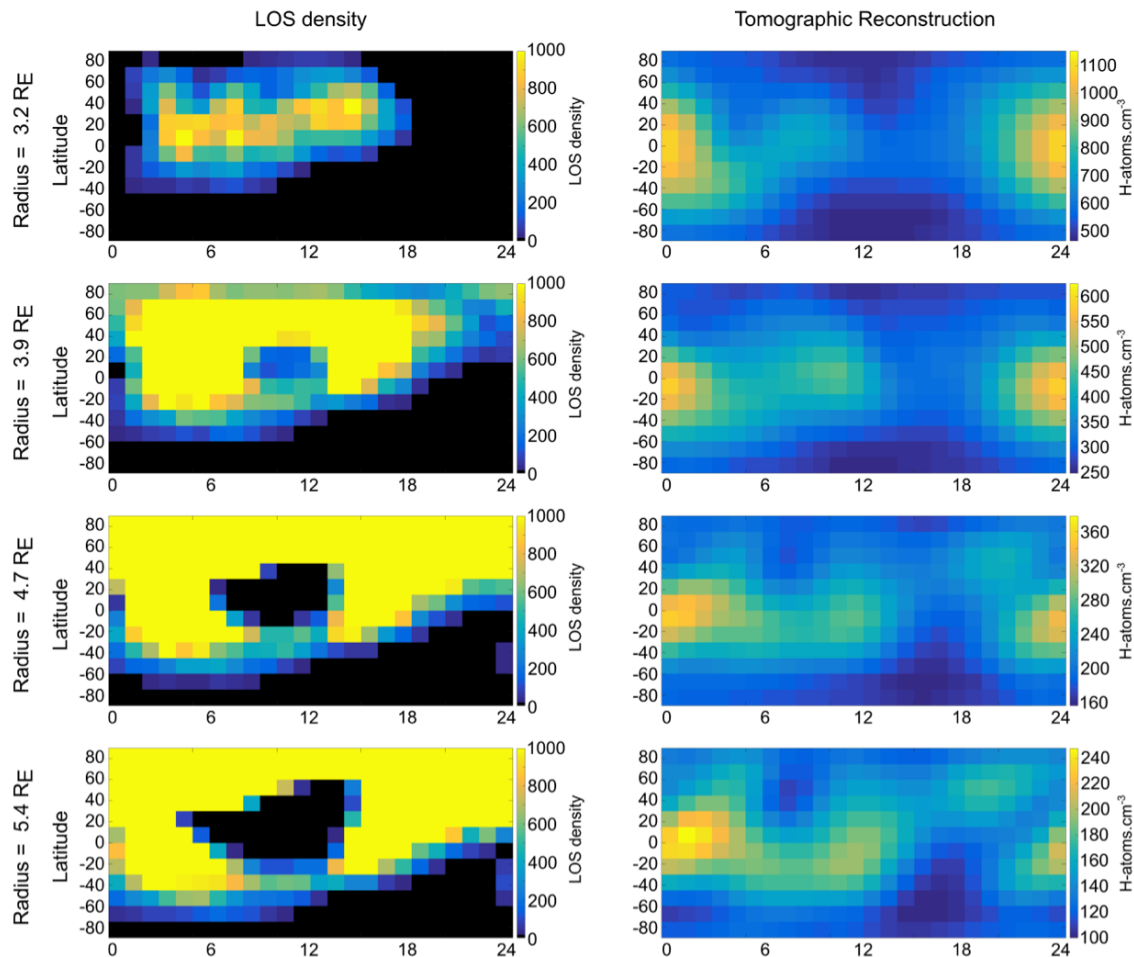
● Static tomographic reconstruction \mathbf{x}^s can be performed during quiet-time conditions using all available data and solving the expression above. During storm-time, a time-dependent model should be used: $\mathbf{y}_k = \mathbf{L}_k \mathbf{x}_k$ such that the input data stream may generate sequential reconstructions \mathbf{x}^d every time k .

● Kalman Filter has been used to estimate the 3-D, time-dependent H density distribution from Ly- α emission. We used a **two-hour period** for reconstructions.

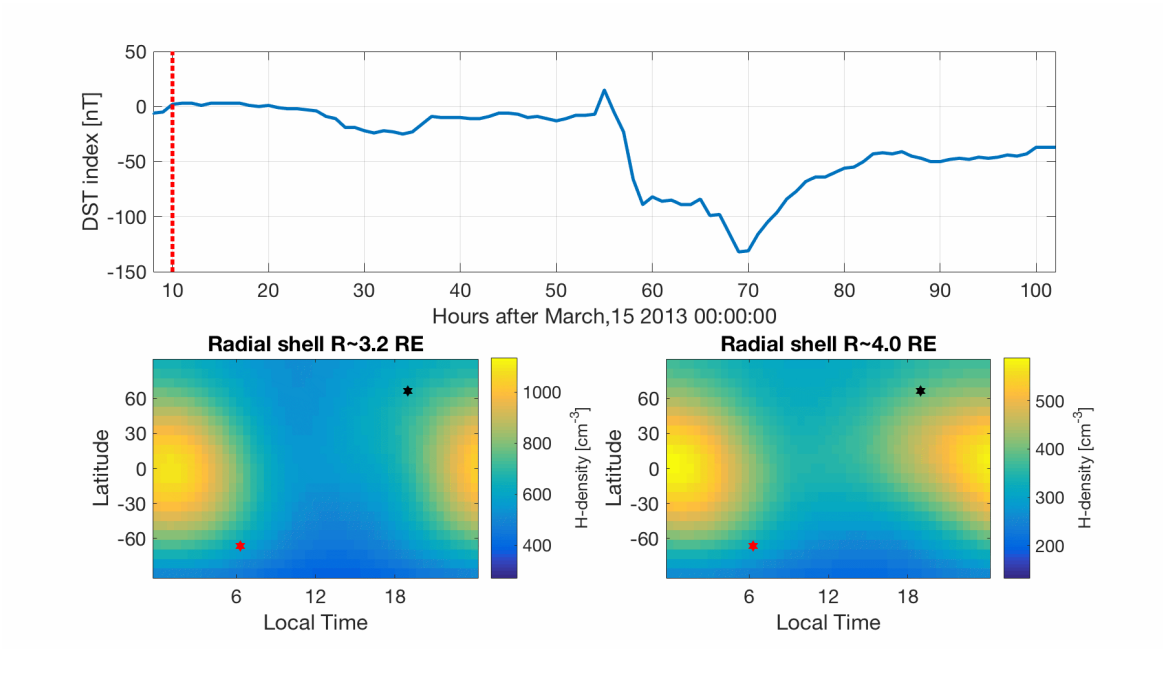
Kalman Filter Algorithm



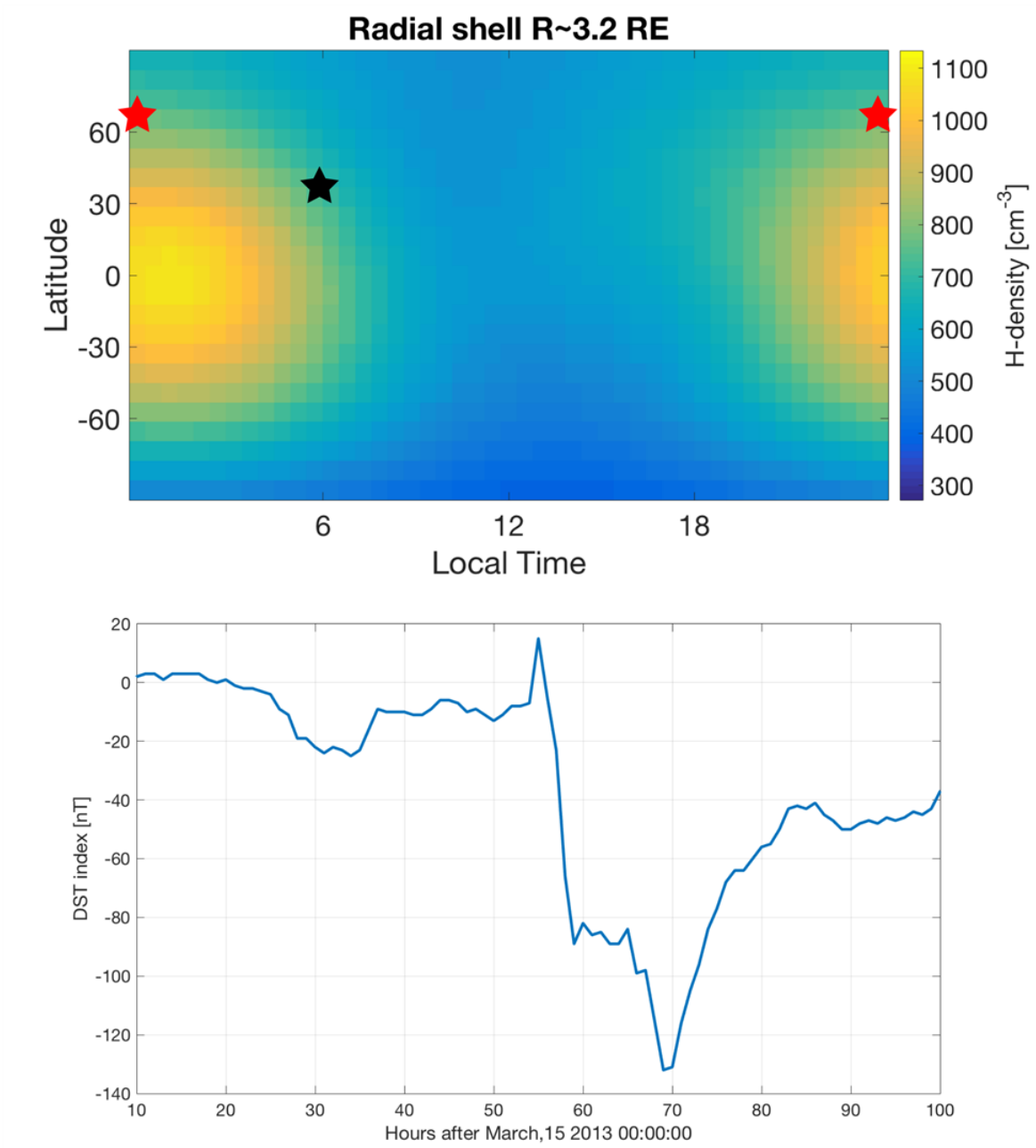
● The initial estimate x^s is obtained by performing a static tomographic reconstruction using TWINS data for October-December 2012 during quiet-time conditions [Cucho-Padin & Waldrop, 2018 (<https://doi.org/10.1029/2018JA025323>)].

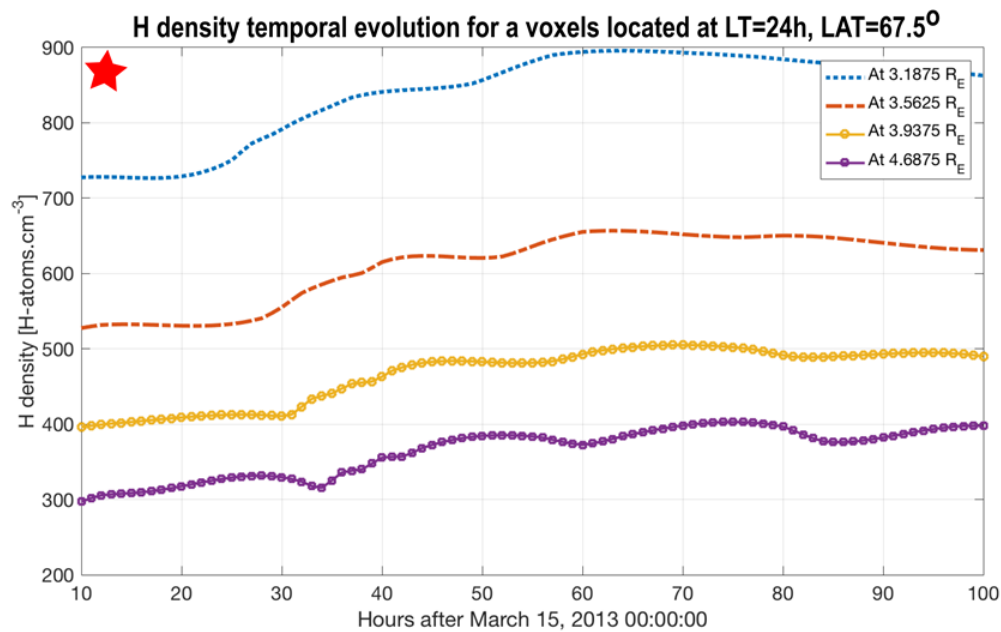
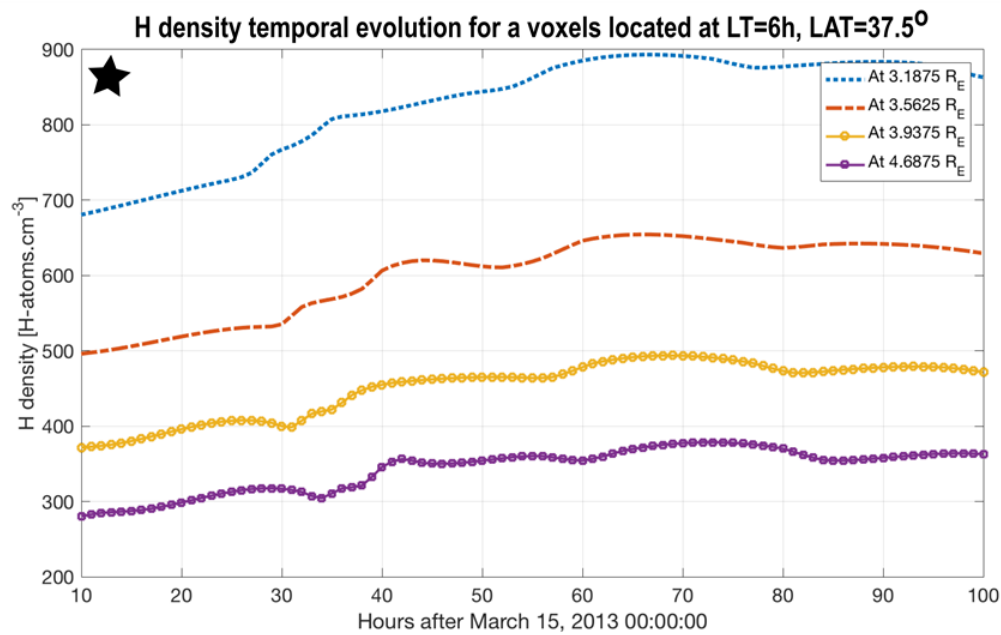


● Dynamic tomographic reconstruction during the storm occurred on March 17, 2013 [Cucho-Padin & Waldrop, 2019 (https://doi.org/10.1029/2019GL084327)].



● Temporal evolution of the H density for selected spatial locations.





Highlights

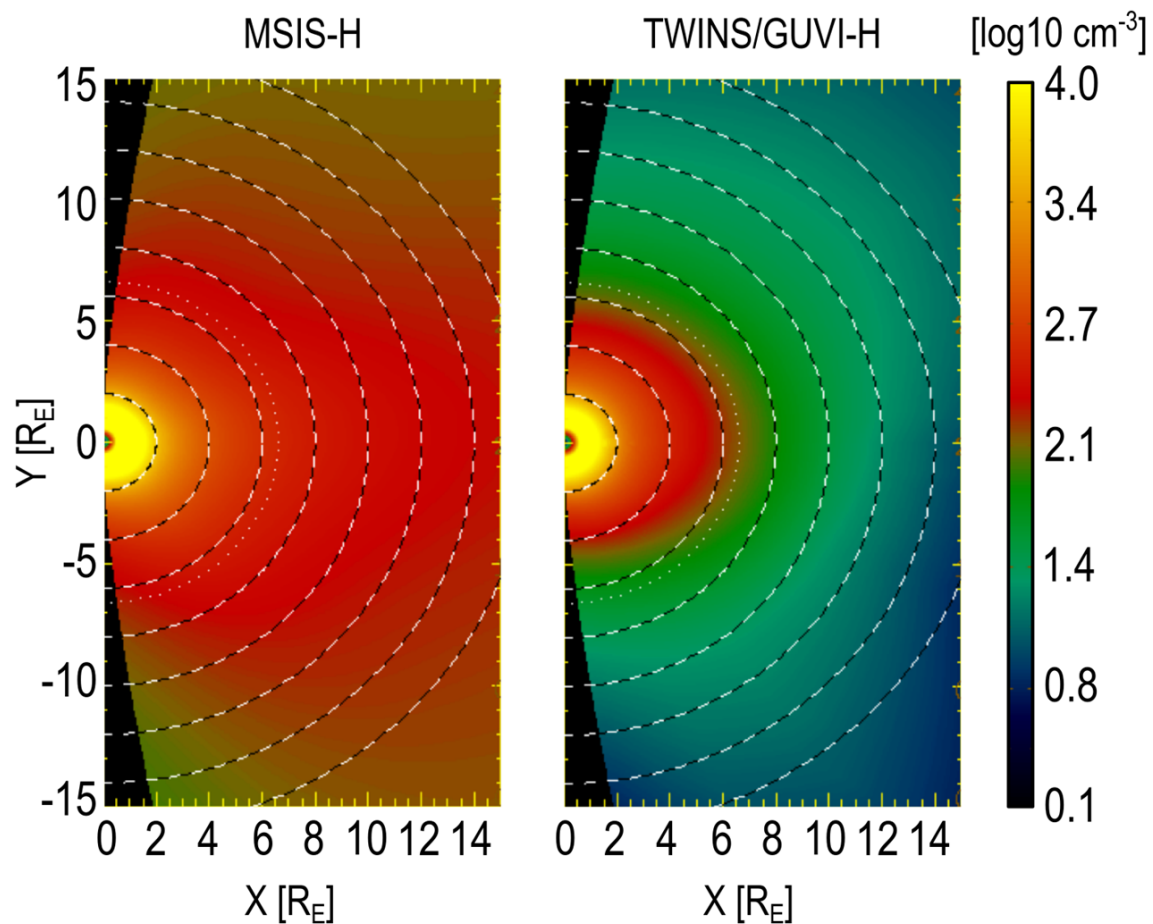
- ✓ The temporal evolution of the H density shows a **~23%** increment (at the peak ~70h after March 15) with respect to quiet-time.
- ✓ Analysis of H density at different altitudes shows an **outward propagation** of H atoms.
- ✓ A constant increment of H density starting at ~30h after March 15 reveals that even **small geomagnetic variations** (DST~-30nT) can trigger an increased H escape.

✓ The balance of injection and loss of H atoms in this region is affected by **exosphere-plasmasphere interaction and thermospheric variations** [Kuwabara et al., 2017 (<https://agupubs.onlinelibrary.wiley.com/doi/full/10.1002/2016JA023247>)]

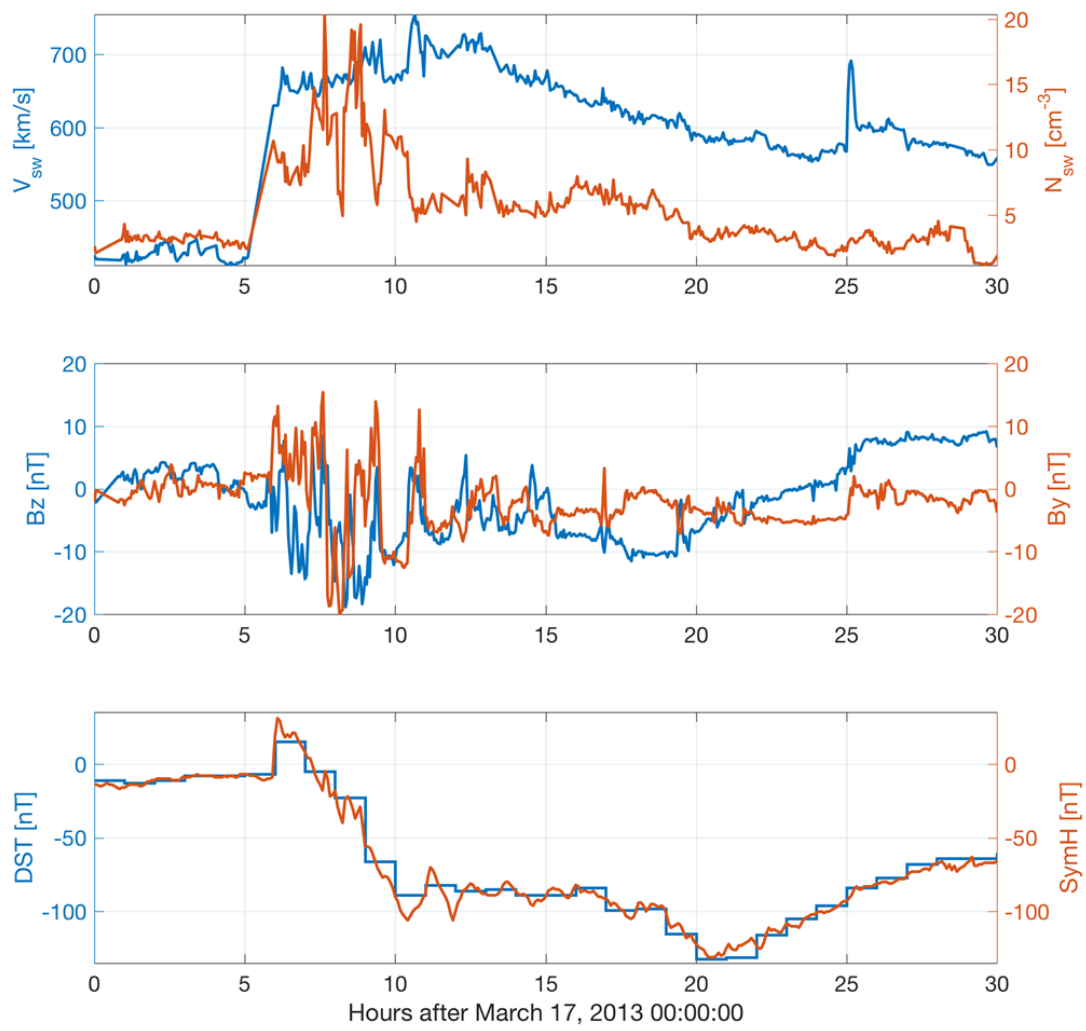
IV. SIMULATIONS OF THE PLASMASPHERE DURING STORM-TIME

Incorporating the dynamic H profile into the IPE model

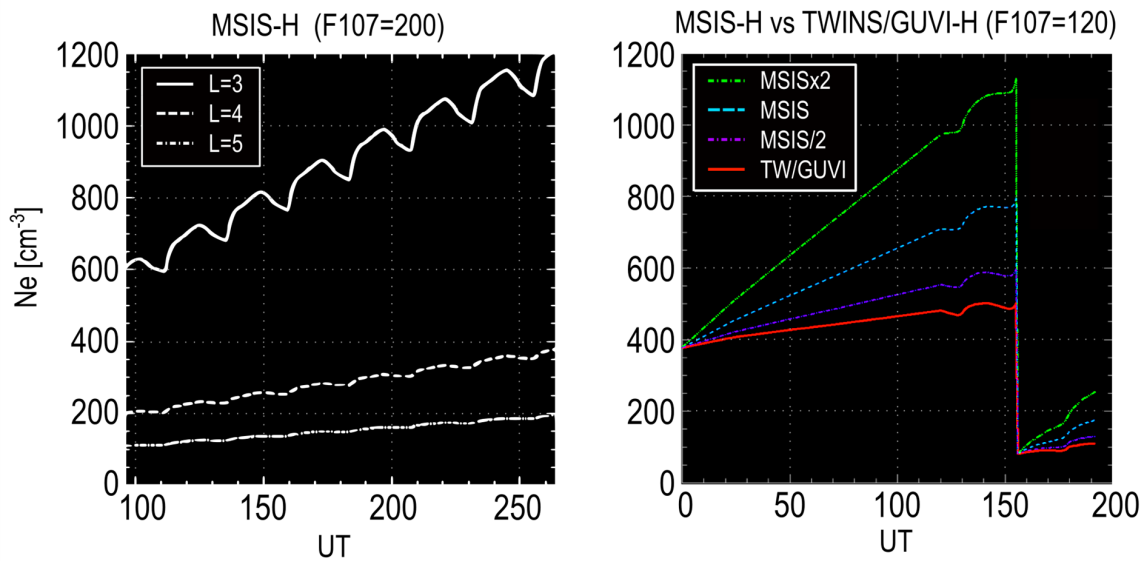
- We analyze the plasmaspheric refilling rate using the H density profile obtained by NRL MSIS-00 and our dynamic H density derived from Ly- α emission (TWINS/GUVI).



- IMF B_z, B_y, solar wind speed V_{sw}, and density N_{sw} measured from the ACE satellite, and DST, SYM-H on **17-18 March 2013**.

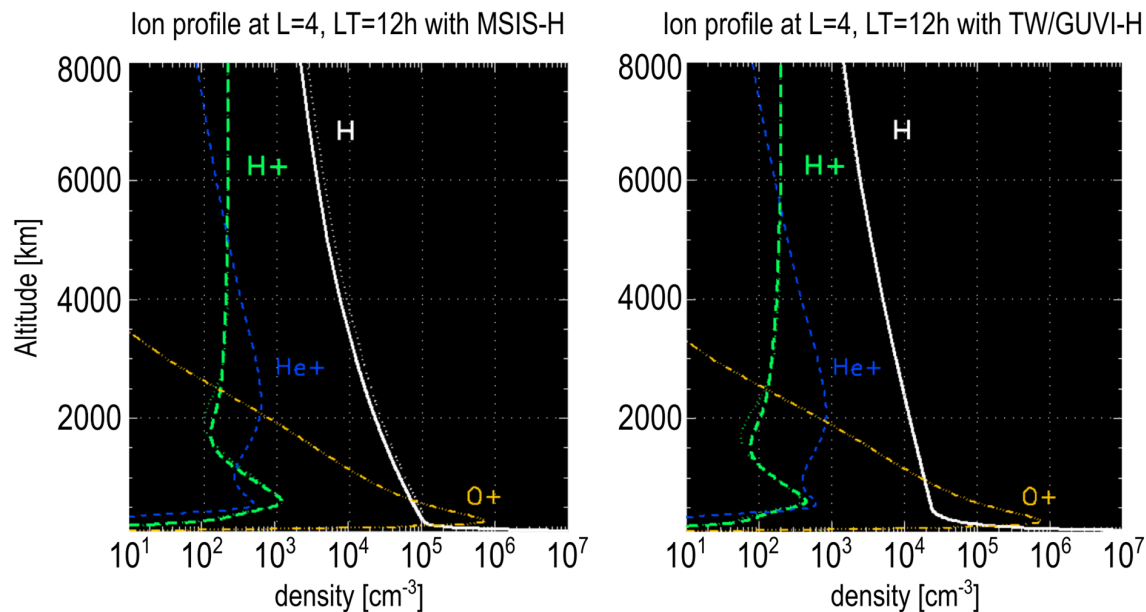


● Refilling rate comparison for two different solar conditions.



The left panel shows the refilling recovery using MSIS H density profile for simulated conditions with $F_{107}=200$. The lines show the temporal evolution of the electron density of a flux tube at $L=3,4,5$ in the American longitude sector.

- Comparison of ion profiles at $L=4$ and $LT=12h$ with both MSIS and TW/GUVI H density profiles.



Highlights

- ✓ Refilling rates identified for default case are:

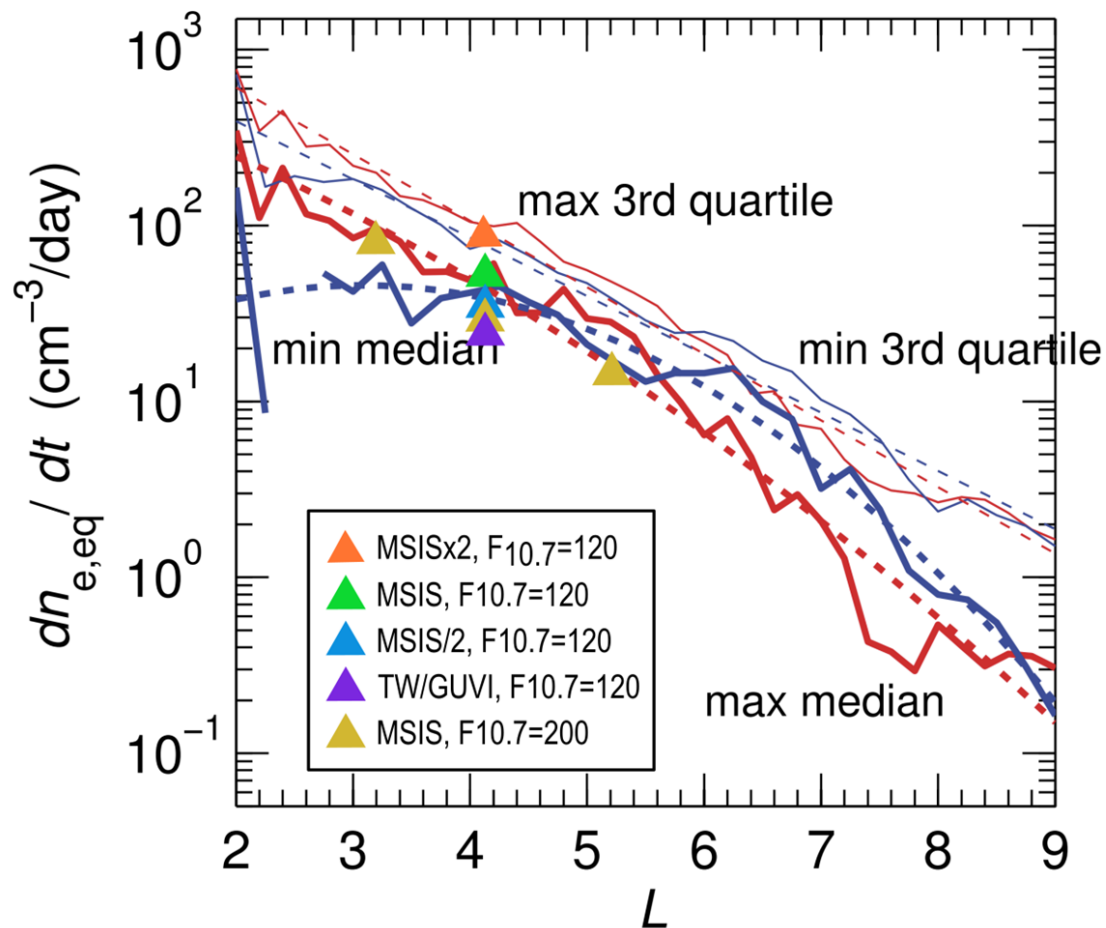
- $L=3$: $89.4 \text{ [cm}^{-3} \cdot \text{d}^{-1}]$
- $L=4$: $25.4 \text{ [cm}^{-3} \cdot \text{d}^{-1}]$
- $L=5$: $12.2 \text{ [cm}^{-3} \cdot \text{d}^{-1}]$

- ✓ Refilling rates identified during March 17, 2013 storm:

- MSISx2 : $99.0 \text{ [cm}^{-3} \cdot \text{d}^{-1}]$
- MSIS : $53.3 \text{ [cm}^{-3} \cdot \text{d}^{-1}]$
- MSIS/2 : $27.2 \text{ [cm}^{-3} \cdot \text{d}^{-1}]$
- TW/GUVI : $19.4 \text{ [cm}^{-3} \cdot \text{d}^{-1}]$

V. REFILLING RATE COMPARISON

- Our refilling rates have good agreement with those reported in [Denton et al., 2012]



Median (thick solid curves) and third quartile (thin solid curves) for the refilling rate $dn_{e,eq}/dt$ during intervals corresponding to solar maximum (red curves) and solar minimum (blue curves). The dotted curves are the corresponding quadratic fits described in the text.

VI. CONCLUSIONS

Conclusions

✓ In this work, we have developed a technique to estimate time-dependent H density from its Ly- α emission. The H density profile has been used to analyze the refilling rate in the plasmasphere during storm-time.

✓ These results emphasize the importance of an accurate estimation of exospheric H density and the need for satellite-based missions to specifically measure the exosphere. The Global Lyman-alpha Imagers for the Dynamic Exosphere (GLIDE) mission led by Dr. Waldrop, has been accepted for launch in 2024. It will provide wide-field global images of the exosphere with a 30-min temporal resolution.

ABSTRACT

As soon as the outer plasmasphere gets eroded during geomagnetic storms, the greatly depleted plasmasphere is replenished by cold, dense plasma from the ionosphere. A strong correlation has been revealed between plasmaspheric refilling rates and ambient densities in the topside ionosphere and exosphere, particularly that of atomic hydrogen (H). Although measurements of H airglow emission at plasmaspheric altitudes exhibit storm-time response, temporally static distributions have typically been assumed in the H density in plasmasphere modeling. In this presentation, we evaluate the impact of a realistic distribution of the dynamic H density on the plasmaspheric refilling rate during the geomagnetic storm on March 17, 2013. The temporal and spatial evolution of the plasmaspheric density is calculated by using the Ionosphere-Plasmasphere Electrodynamics (IPE) model, which is driven by a global, 3-D, and time-dependent H density distribution reconstructed from the exospheric remote sensing measurements by NASA's TWINS and TIMED missions. We quantify the spatial and temporal scales of the refilling rate and its correlation with H densities.

REFERENCES

- Krall, J., Gloer, A., Fok, M.-C., Nossal, S. M., & Huba, J. D. (2018). The unknown hydrogen exosphere: Space weather implications. *Space Weather*, 16, 205–215. <https://doi.org/10.1002/2017SW001780>
- Bailey, J., and Gruntman, M. (2011), Experimental study of exospheric hydrogen atom distributions by Lyman- α detectors on the TWINS mission, *J. Geophys. Res.*, 116, A09302, doi:10.1029/2011JA016531.
- Zoennchen, J. H., et al. (2015) "Terrestrial exospheric hydrogen density distributions under solar minimum and solar maximum conditions observed by the TWINS stereo mission." *Annales Geophysicae*, vol. 33, no. 3, p. 413.
- Hodges, R. R. (1994), Monte Carlo simulation of the terrestrial hydrogen exosphere, *J. Geophys. Res.*, 99(A12), 23229–23247, doi:10.1029/94JA02183.
- Zoennchen, J. H., Nass, U., Fahr, H. J., and Goldstein, J.: The response of the H geocorona between 3 and 8 Re to geomagnetic disturbances studied using TWINS stereo Lyman- α data, *Ann. Geophys.*, 35, 171–179, <https://doi.org/10.5194/angeo-35-171-2017>, 2017.
- Kuwabara, M., Yoshioka, K., Murakami, G., Tsuchiya, F., Kimura, T., Yamazaki, A., and Yoshikawa, I. (2017), The geocoronal responses to the geomagnetic disturbances, *J. Geophys. Res. Space Physics*, 122, 1269–1276, doi:10.1002/2016JA023247.
- McComas, D.J., Allegrini, F., Baldonado, J. et al. (2009) The Two Wide-angle Imaging Neutral-atom Spectrometers (TWINS) NASA Mission-of-Opportunity. *Space Sci Rev* 142, 157–231. <https://doi.org/10.1007/s11214-008-9467-4>
- Qin, J., Waldrop, L., and Makela, J. J. (2017), Redistribution of H atoms in the upper atmosphere during geomagnetic storms, *J. Geophys. Res. Space Physics*, 122, 10,686–10,693, doi:10.1002/2017JA024489.
- Østgaard, N., Mende, S. B., Frey, H. U., Gladstone, G. R., and Lauche, H. (2003), Neutral hydrogen density profiles derived from geocoronal imaging, *J. Geophys. Res.*, 108, 1300, doi:10.1029/2002JA009749, A7.
- Cucho-Padin, G., & Waldrop, L. (2018). Tomographic estimation of exospheric hydrogen density distributions. *Journal of Geophysical Research: Space Physics*, 123, 5119–5139. <https://doi.org/10.1029/2018JA025323>
- Cucho-Padin, G., & Waldrop, L. (2019). Time-dependent response of the terrestrial exosphere to a geomagnetic storm. *Geophysical Research Letters*, 46, 11661–11670. <https://doi.org/10.1029/2019GL084327>
- Rairden, R. L., Frank, L. A., and Craven, J. D. (1986), Geocoronal imaging with Dynamics Explorer, *J. Geophys. Res.*, 91(A12), 13613–13630, doi:10.1029/JA091iA12p13613.